AGRIVITA Journal of Agricultural Science. 2023. 45(2): 296–310

AGRIVITA
Journal of Agricultural Science
www.agrivita.ub.ac.id

# Optimization of Aquaponic Lettuce Evapotranspiration Based on Artificial Photosynthetic Light Properties Using Hybrid Genetic Programming and Moth Flame Optimizer

**Mary Grace Ann Bautista[1*], Ronnie Concepcion II[2], Argel Bandala[1], Christan Hail Mendigoria[1], and Elmer Dadios[2]**

[1] Department of Electronics and Computer Engineering, De La Salle University, Manila, Philippines
[2] Department of Manufacturing Engineering and Management, De La Salle University, Manila, Philippines

**ARTICLE INFO**

*Keywords:*
Aquaponic lettuce
Artificial light properties
bio-inspired optimization
Evapotranspiration rate
Genetic programming

*Article History:*
**Received: May 12, 2022**
**Accepted: June 8, 2023**

*) Corresponding author:
E-mail: mary_grace_bautista@dlsu.edu.ph

**ABSTRACT**

Land and water resources, climate change, and disaster risks significantly affect the agricultural sector. An effective solution for growing crops to improve productivity and optimize the use of resources is through controlled-environment agriculture (CEA). Evapotranspiration (ET) is an important greenhouse crop attribute that can be optimized for optimum plant growth. Light intensity and radiation are significant for controlling ET. To address this challenge, this study successfully determined the properties of optimum artificial light for minimum evapotranspiration rate of head development-stage and harvest-stage lettuce under light-period and dark-period using genetic programming and bio-inspired algorithms namely, grey wolf optimization (GWO), whale optimization algorithm (WOA), dragonfly algorithm (DA), and moth flame optimization (MFO). MFO provided the optimized global solution for the configured models. Results showed that head development-stage lettuce requires higher light intensity with lower visible to infrared radiation ratio (Vis/IR) than harvest-stage lettuce when exposed to light. On the other hand, harvest-stage lettuce requires higher light intensity with lower Vis/IR than head development-stage under dark-period respiration reaction. Findings of this study can be utilized in growing and improving yield crops in controlled-environment agriculture.

## INTRODUCTION

Covid19 pandemic and community quarantines emphasize food security and resiliency in the new normal. In the Philippines, the agriculture sector continuously addresses persistent challenges, including the constraints to land and water resources access, vulnerability to climate changes, global warming, and disaster risks to ensure the availability, accessibility, and affordability of nutritious food to achieve a healthy and resilient community (National Economic Development Authority, 2017). Controlled-environment agriculture (CEA) is an effective solution for growing crops under managed environments while improving productivity and optimizing resource use (Benke & Tomkins, 2017). Regulation of light intensity, carbon dioxide concentration, temperature and humidity level, and photoperiod can be made in CEA to improve crop production (Valenzuela et al., 2017; Valenzuela et al., 2018; Concepcion et al., 2021; Cammarisano et al., 2019). Several studies optimized nutrients from the soil that contains Nitrogen (N), phosphorous (P), and potassium (K) for lettuce. Commonly grown crops in the CEA greenhouse includes lettuce, cucumber, tomato, and pepper (J. Zou et al., 2020; Ke et al., 2021; Kwack et al., 2021).

Among these factors, optimizing plant growth by enabling the most desirable lighting conditions for a certain crop at different developmental stages was recently explored. The emitting diode (LED) of a sun-like light that simulates the natural solar spectrum allows intensity modulation and light

**ISSN: 0126-0537**

***Cite this as:*** Bautista, M. G. A., Concepcion II, R., Bandala, A., Christan, H. M., & Dadios, E. (2023). Optimization of aquaponic lettuce evapotranspiration based on artificial photosynthetic light properties using hybrid genetic programming and moth flame optimizer. *AGRIVITA Journal of Agricultural Science*, *45*(2), 296–310. http://doi.org/10.17503/agrivita.v45i2.3786

spectrum composition. LED lights consume less energy compared to traditional light sources and operate in lower temperatures (Loconsole et al., 2019). Several studies have reported the effects of light in enhancing plant growth. Red and blue light were identified as the preeminent light spectrum for plant growth and development (Chen et al., 2017). Red light increases the concentration of phenolics in lettuce (Lee et al., 2016), while blue light is efficiently effective in stimulating biomass, sucrose, and starch accumulation, photomorphogenesis, as well as accelerated carboxylation (Chen et al., 2017; Chen et al., 2019; Tarakanov et al., 2022). Another study indicates that LED light with the red and blue spectrum and low irradiance can significantly improve lettuce yield and antioxidant activity (Mohamed et al., 2021). Greenhouse plant photomorphogenesis is positively affected by Far-red (FR) light (Kump, 2020), meanwhile, a remarkable decrease in stomatal density is the result of monochromatic red and blue lights (Izzo et al., 2021). Also, the humidity and temperature of the air are affected by red-blue and yellow spectrums (Marcos & Mai, 2020). The 15 hours of photoperiod combined with red-blue light (4:1) resulted in a positive impact on spinach (T. Zou et al., 2020). The dark-period respiration of 22 hours and 15 light hours of consecutive photoperiod resulted in a low starch content in the leaf which is an indication of an increase in the photosynthetic rate (Urairi et al., 2017). Effects of light intensity and distance to crops were also reported to influence growth and plant structure (Lee et al., 2016; Camejo et al., 2020).

Consequently, little information is available on the effects of the intensity of light in the optimization of the evapotranspiration of plants. Evapotranspiration (ET) is another important attribute of greenhouse crops for significant quality and value, especially for lettuce. ET is the loss of water from vegetation through combined processes of surface evaporation and plant transpiration. It is well known that light intensity and radiation play an important role in the determination of water loss from plants. A physiological disorder of lettuce known as tip burn has been linked to insufficient evapotranspiration (Périard et al., 2015).

Elucidating the effects of the artificial light and its properties on the ET rate of aquaponic green loose-leaf lettuce are the focus of this study. The artificial light properties include distance, light intensity, infrared radiation, and visible radiation, and they shall be analyzed to optimize their effect using hybrid genetic programming and Moth Flame Optimization (MFO) algorithm, Grey Wolf Optimizer (GWO), Whale Optimization Algorithm (WOA), and Dragonfly Algorithm (DA) were also explored for the optimization process. The use of these swarm intelligence metaheuristic techniques to find the global optimum value of parameters has been deeply explored. These algorithms have proven track of optimizing nonlinear conditions (Monga et al., 2021; Darwish, 2018). GWO algorithm is based on grey wolves' hierarchy of leadership, the alpha, beta, delta, and omega. In addition, their hunting mechanism is also implemented in this algorithm (Darwish, 2018). WOA is based on the social behavior of humpback whales and their hunting strategy (Mirjalili & Lewis, 2016). DA originates from the swarming behaviors of dragonflies in nature. Optimization is designed by modeling navigation, foraging, and enemy avoidance of dragonflies when swarming dynamically or statistically (Darwish, 2018). MFO is inspired by the navigation method of moths to fly in the direction of moonlight called transverse orientation. In solving optimization problems, the mathematical model of the spiral flying path of moths around artificial flames or lights is used (Mirjalili, 2015). The results of this study can be utilized in growing and improving yield crops in a controlled environment and can be promisingly applied in commercial scale. This study contributes to the: (1) understanding of the impacts of artificial photosynthetic light properties like light intensity, infrared radiation and visible radiation to photosynthetic and respiration rate of aquaponic lettuce; and (2) development of hybrid computational intelligence models in optimizing the distance of light source and light properties to lettuce leaf canopy in which varied at head development and harvesting stage that induces crop primary growth inside a controlled environment.

## MATERIALS AND METHODS

The data collection for this study was conducted in a smart lettuce farm located at Morong, Rizal, Philippines in June 2021.The first stage of the study was the measurement of the properties of the artificial light (distance of the light source, light intensity, infrared radiation, and visible radiation). It was followed by the leaf disk floatation assay to determine the photosynthetic and respiration rate of the aquaponic lettuce. Further, this study included

the development of bioinspired optimization models to optimize the evapotranspiration based on artificial light properties to improve lettuce growth (Fig. 1) (Bautista et al., 2022).

**Controlled Environment Condition**

Green loose-leaf lettuce was used in the study, since it has been reported to be dependent and significantly affected by various environmental conditions. In a smart farm located at Morong, Rizal, Philippines, the cultivar was subjected to nutrient film technique (NFT) for 6 weeks. The growing bed was maintained with 124.70 mg/l nitrate, potassium of 168.74 mg/l, and phosphate of 65.23 mg/l, wherein electrical conductivity and pH level were controlled between 1 ± 0.02 mS/cm and 6 ± 0.5, respectively (Concepcion et al., 2021; Bautista, et al., 2022).

**Measurement of the Artificial Light Properties**

A 67449.16 $cm^3$ (35.56 x 35.56 x 53.34 cm) black plastic tray was used as the closed chamber, wherein an aluminum foil was placed inside to cover its wall surface. This technique enabled the light from the artificial photosynthetic light source to reflect inside the chamber. The chamber used a monochromatic light source that could easily be attached, used, and detached, with a 10, 20, and 30 cm distance from the bottom of the plastic container (Fig. 2a). Red, orange, yellow, white, green, blue, and violet light spectrums were used with 32 W, 190 ± 5 μmol/$m^2$/s photosynthetic photon flux density (PPFD) (Firefly, Ace Hardware Corp., Philippines) (Fig. 2b). In the 30, 20, and 10 cm segments, 3 light intensity sensors (Adafruit TSL2561, China) were placed to determine the light intensity, infrared, and visible radiations varied by the distance of the light source to the disk container and differentiated by each light spectrums. In the optimization analysis, these gathered spectral data were likewise used (Concepcion et al., 2021; Bautista, et al., 2022).

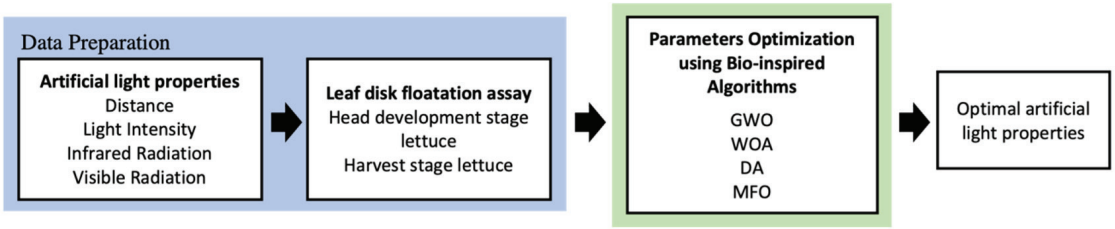


**Fig. 1.** Developmental architecture of optimizing artificial light properties of aquaponic lettuce (distance, light intensity, infrared and visible radiation) using bioinspired algorithms

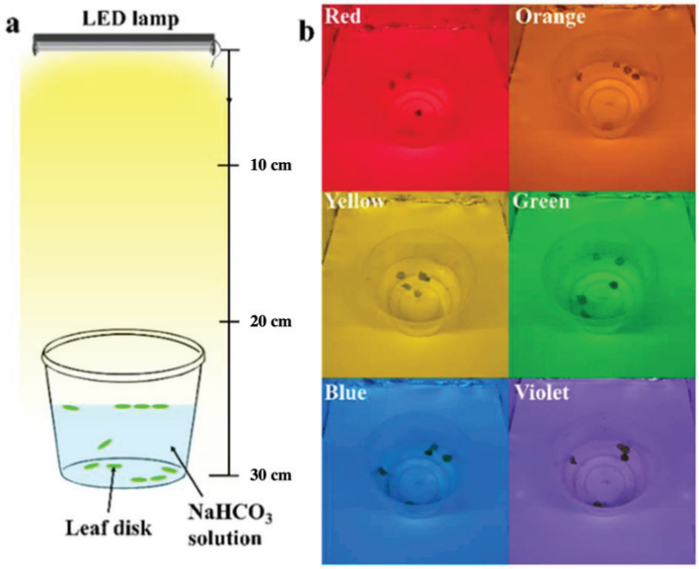


**Fig. 2.** (a) Proximity of the artificial photosynthetic light source from the leaf disk floatation container and (b) the captured images of the actual monochromatic light spectrum's resemblance for the closed chamber adapted from Concepcion et al., (2021)

**Leaf Disk Floatation Assay**

This study used leaf disk floatation to determine the photosynthetic and respiration rate of both the head development and harvest-stage aquaponic lettuce. The test was performed by mixing 0.425 g of $NaHCO_3$ with 300 ml of distilled water to produce a 0.2% sodium bicarbonate ($NaHCO_3$) solution. To wet the hydrophobic leaf surface, a drop of liquid soap was added. Ten uniform leaf disks from head development-stage and harvest-stage aquaponic leaves of lettuce were cut using plastic straw measuring 1 cm in diameter, avoiding leaf veins and midrib. Thereafter, a 5 $cm^3$ of $NaHCO_3$ solution was put inside the barrel of syringe with 10 $cm^3$, where leaf disks were placed later. To make the leaf disks infiltrated with the solution, a small vacuum was placed inside the syringe. Thereafter, the plunger and leaf disks were removed upon sinking thereof on the bottom of the syringe. The leaf disks were placed in a clear plastic floatation container which was prepared with the same bicarbonate solution. Under the fluorescent lamp with the proximity of 30 cm, the clear plastic floatation container was placed for photosynthetic reaction. Upon exposure of the container, the timer started, and the floating disks count were recorded for every minute. The experiment continued until all the leaf disks were floated. Subsequently, floatation container was put inside a box without light source to perform the dark-period aerobic respiration, and the floating disks count were also recorded for every minute (Concepcion et al., 2021; Bautista, et al., 2022).

There were 42 trials for photosynthesis and a corresponding 42 trials for respiration based on the 7 artificial monochromatic lights (red, orange, yellow, white, green, blue, and violet), 2 lettuce leaf maturities (head development-stage and harvest-stage), and 3 light source proximities (10, 20, and 30 cm) (Concepcion et al., 2021; Bautista, et al., 2022).

The photosynthetic rate ($1/ET_{50\text{-}light}$) and respiration rate ($1/ ET_{50\text{-}dark}$) were calculated using the eqn. 1 and 2.

$$\frac{1}{ET_{50-light}} = \frac{1}{t_{50\%-l}} \quad \text{..... (1)}$$

$$\frac{1}{ET_{50-dark}} = \frac{1}{t_{50\%-d}} \quad \text{..... (2)}$$

where: $t_{50\%-l}$ is the time (in minutes) during the light period when half of the total leaf disks are floating while $t_{50\%-d}$ is the time during the dark period.

**Bioinspired Evapotranspiration Optimization Models**

Aquaponic lettuce growth was affected by combination of nonlinear artificial light properties in terms of evapotranspiration rate. Thus, to determine the best combination, there was a need to develop an effective bioinspired minimization optimization model. The regression model for the objective functions were generated using multigene symbolic regression genetic programming (MSRGP).

MSRGP was an evolutionary algorithm in MATLAB under the GPTIPS2 application. It was configured with 100 maximum generations, 1000 population size, 4 for tournament size, 0.10 elite fraction, maximum of 10 genes, 0.05 probability of pareto tournament, maximum tree depth of 5, 0.84 for crossover rate with mutation rate of 0.14, and would terminate when fitness value < 0.001.

In this study, the objective function were named as follows: HDL (per minute), resembled the ET rate for head development-stage lettuce during light period; HL (per minute), resembled the ET rate for harvest-stage lettuce during light period; HDD (per minute), resembled the ET rate for head development-stage lettuce during dark period; and HD (per minute), resembled the ET rate for harvest-stage lettuce during dark period. These were functions of the light distance in centimeter ($x_1$), and artificial light properties in μmol/$m^2$/s, namely, infrared radiation ($x_2$), light intensity ($x_3$), and visible radiation ($x_4$) (Bautista, et al., 2022).

The configured model achieved $R^2$ of 0.974, 0.970, 0.924, and 0.988 for HDL, HL, HDD, and HD, respectively. (Eqn. 3-6)

$$\begin{aligned} HDL &= f(x_1, x_2, x_3, x_4) \quad \text{..... (3)} \\ &= 0.00297\, sin(x_1) - 5.85x10^{-6}x_3 - 0.0424abs\left(sin\left(\sqrt{x_2}\right)\right) \\ &\quad -2.15x10^{-6}\, abs(x_2) - 2.92x10^{-6}\, abs(x_3) - 2.15x10^{-6}\, x_2 \\ &\quad +0.0197\, sin(x_2) + 2.43x10^{-6}\, x_1x_4 - 0.0399\sqrt{x_1} + 0.179 \end{aligned}$$

$$\begin{aligned} HL &= f(x_1, x_2, x_3, x_4) \quad \text{..... (4)} \\ &= 5.24x10^{-5}x_3 - 3.99x10^{-5}\, x_4 + 0.00297abs(2.0x_1 + 9.0) \\ &\quad -0.0148\cos(x_2{}^2) + 0.0535\sin(sin(x_2)) - 1.04x10^{-4}abs(x_1) \\ &\quad -2.27x10^{-5}\, abs(x_4) + 9.58x10^{-6}\cos(x_2) + 1.55x10^{-6}x_1x_4 \\ &\quad +3.54x10^{-4} \end{aligned}$$

$$\begin{aligned} HDD &= f(x_1, x_2, x_3, x_4) \quad \text{..... (5)} \\ &= 2.85x10^{-4}x_2 - 1.88x10^{-4}x_1 + 3.52x10^{-5}x_4 \\ &\quad -0.00813\cos(x_1 + 0.416) - 5.86x10^{-4}\cos(x_1 + x_2) \\ &\quad -7.7x10^{-5}\sin(x_2) - 1.88x10^{-4}\sqrt{x_2}\,\sqrt{x_3} \\ &\quad +4.55x10^{-4}x_1\sin(2.0x_3) + 0.0263 \end{aligned}$$

$$\begin{aligned} HD &= f(x_1, x_2, x_3, x_4) \quad \text{..... (6)} \\ &= 4.73x10^{-4}x_1 - 6.94x10^{-6}x_2 + 1.19x10^{-6}x_4 + 0.00166\cos(2.0x_2) \\ &\quad -8.76x10^{-4}\sin(x_2x_3) + 0.00249\log(\log(1/x_3) + x_2{}^3) \\ &\quad -0.00215\sin(x_4) - 1.03x10^{-6}abs\sqrt{(x_2(x_1x_3 - 1.0))} - 0.0235 \end{aligned}$$

Bioinspired algorithms including GWO, WOA, DA, and MFO were explored. These algorithms had a proven track on optimizing nonlinear conditions (Darwish, 2018).

**Grey Wolf Optimization (GWO) Algorithm**

GWO algorithm represented the mathematical model of the social hierarchy of wolves where the fittest solution was alpha (α), second best solution was beta (β), delta (δ) as the third best solution, while the rest of the remaining solutions were assumed to be omega (ω) (Darwish, 2018).

The encircling behavior of wolves was modeled as: (Eqn. 7-8)

$$\vec{D} = \left|\vec{C}.\vec{X}_p(t) - \vec{X}(t)\right| \quad (7)$$

$$\vec{X}(t+1) = \vec{X}_p(t) - \vec{A}.\vec{D} \quad (8)$$

Where: t is the iteration, $\vec{A}$ and $\vec{C}$ are coefficient vectors, $\vec{X}_p$ represents the position of the prey, and $\vec{X}$ for the position of a wolf.

The coefficient vectors were computed using eqn. 9-10

$$\vec{A} = 2\vec{a}.\vec{r}_1 - \vec{a} \quad (9)$$

$$\vec{C} = 2.\vec{r}_2 \quad (10)$$

Where: components of $\vec{a}$ are linearly decreased from 2 to 0 over the course of iterations and $\vec{r}_1$, $\vec{r}_2$ are random vectors in [0, 1].

The mechanism of this algorithm was based on determining the α, β, δ and positions. To describe their hunting behavior, the first alpha, beta, and delta solutions were stored, then positions were updated with respect to the position of the best search agent described by the mathematical forms (Eqn 11-14):

$$\vec{D}_\alpha = \left|\vec{C}_1.\vec{X}_\alpha - \vec{X}\right|, \vec{X}_1 = \vec{X}_\alpha - \vec{A}_1.\left(\vec{D}_\alpha\right) \quad (11)$$

$$\vec{D}_\beta = \left|\vec{C}_2.\vec{X}_\beta - \vec{X}\right|, \vec{X}_2 = \vec{X}_\beta - \vec{A}_2.\left(\vec{D}_\beta\right) \quad (12)$$

$$\vec{D}_\delta = \left|\vec{C}_3.\vec{X}_\delta - \vec{X}\right|, \vec{X}_3 = \vec{X}_\delta - \vec{A}_3.\left(\vec{D}_\delta\right) \quad (13)$$

$$\vec{X}(t+1) = \frac{\vec{X}_1 + \vec{X}_2 + \vec{X}_3}{3} \quad (14)$$

The value of $\vec{a}$ linearly decreased to quantifiably model the behavior of wolves approaching their prey. In this case, $\vec{A}$ would be a random value in the interval [-*2a*, *2a*] where *a* was decreased from 2 to 0. When the random values of $\vec{A}$ were in [-1, 1] provided that |A|<1, then the algorithm enabled the wolves to attack their prey (Darwish, 2018).

To summarize, the algorithm started by initializing the grey wolf population or the number of search agents. It was followed by the calculation of the fitness for the first three best solutions, $X_\alpha$, $X_\beta$, and $X_\delta$ and position update of other search agents based on the best search agents position. Coefficients vectors A and C would be updated to calculate the new fitness for the best solutions of the next iteration until the maximum iteration or optimal solution was met. The final fitness value of the best search agent $X_\alpha$ would be returned as the global best solution (Darwish, 2018).

**Whale Optimization Algorithm (WOA)**

The whale optimization algorithm was based on the behavior of humpback whales called as the bubble-net feeding method. It was assumed that the target prey was the current best candidate solution. Once the best search agent was determined, other search agents would update their positions towards the prey (Mirjalili & Lewis, 2016). This behavior was defined by the following Eqn. 15-16

$$\vec{D} = \left|\vec{C} * \vec{X}'(t) - \vec{X}(t)\right| \quad (15)$$

$$\vec{X}(t+1) = \vec{X}'(t) - \vec{A} * \vec{D} \quad (16)$$

Where: t refers to the position iteration, $\vec{A}$ and $\vec{C}$ are coefficient vectors, $\vec{X}'$ is the position of the current optimal solution, $\vec{X}$ is the position, | | is the absolute value, and * is an element-by-element multiplication (Darwish, 2018).

Coefficient vectors were evaluated by Eqn. 17-18

$$\vec{A} = 2\vec{a}.\vec{r} - \vec{a} \quad (17)$$

$$\vec{C} = 2\vec{r} \quad (18)$$

Where: $\vec{a}$ is selected from 2 to 0, and $\vec{r}$ as a random vector in the interval of [0, 1] (Darwish, 2018).

The humpback whale's bubble-net phase could be described in a mathematical model using the shrinking encircling method and the spiral updating position method. Using the first method, $\vec{A}$ was decreasing and randomly selected in the [-*a, a*] interval, where *a* was also decreased from 2 to 0 during iterations (Darwish, 2018; Mirjalili & Lewis, 2016). On the other hand, a spiral equation could be used to evaluate the position of the whale and prey through the spiral updating position method using eqn. 19

$$\vec{X}(t+1) = \vec{D}' * e^{bi}\cos(2\pi l) + \vec{X}'(t) \quad (19)$$

Where: $\vec{D}' = \vec{X}'(t) - \vec{X}(t)$ pertains to the distance of *i*th whale to its prey, *b* is a constant, and *l* is a random number in the interval of [-1, 1], and * for element-by-element multiplication.

In the optimization phase, humpback whales were swimming around their prey in a shrinking circle pattern with the probability of 0.5% for position update using a spiral model (Mirjalili & Lewis, 2016). Thus, the eqn. 20 could be used to mathematically describe whale's behavior:

$$\vec{X}(t+1) = \begin{cases} \vec{X}'(t) - \vec{A}.\vec{D} & if\ p < 0.5 \\ \vec{D}' * e^{bi}\cos(2\pi l) + \vec{X}'(t) & if\ p \geq 0.5 \end{cases} \quad \text{.... (20)}$$

Where: p is a random value in the interval of [0, 1].

For the search for prey phase, $\vec{A}$ was defined with random values greater than 1 or less than -1. This mechanism with $|\vec{A}| > 1$ enabled performing global search, and was modeled mathematically using eqn. 21-22.

$$\vec{D} = \left|\vec{C}.\vec{X}_{rand} - \vec{X}\right| \text{..... (21)}$$

$$\vec{X}(t+1) = \vec{X}_{rand} - \vec{A}.\vec{D} \text{..... (22)}$$

Where: $\vec{X}_{rand}$ is a random position vector.

In summary, WOA started the searching process based on the solutions that were randomly selected. Search agents would update their positions based on the obtained best solution. The *a* parameter was decreased from 2 to 0 for exploration and exploitation. A random search agent was chosen when $|\vec{A}|$ was greater than 1 while the best solution was selected when $|\vec{A}|$ was less than 1. The algorithm could switch between spiral or circular movement depending on the value of *p* and would stop by satisfying the termination criterion (Darwish, 2018; Mirjalili & Lewis, 2016).

**Dragonfly Algorithm (DA**

Dragonfly algorithm was based on the behavior of swarms which followed the principles of separation, alignment, and cohesion. It was also based on the concept of survival where all should be attracted towards food sources and distracted outward enemies (Darwish, 2018). The behavior of dragonflies was modeled based on these five patterns, and modeled as eqn. 23-27

Separation : $S_i = -\sum_{j=1}^{N} X - X_j$ ..... (23)

Alignment : $A_i = \frac{\sum_{j=1}^{N} V_j}{N}$ ..... (24)

Cohesion : $C_i = \frac{\sum_{j=1}^{N} X_j}{N} - X$ ..... (25)

Attraction to food : $F_i = X^+ - X$ ..... (26)

Distraction from enemy : $E_i = X^- - X$ ..... (27)

Where: $X$ is the position of the current individual, $X_j$ shows the position of the *j*th neighboring individual, $V_j$ shows the velocity of the *j*th neighboring individual, $X^+$ is the position of the food source, $X^-$ is the position of the enemy, and $N$ is the number of neighboring individuals (Darwish, 2018).

To update the position of artificial dragonflies in a search space, step ($\Delta X$) and position ($X$) vectors were considered. The step vector showed the direction of their movement and could be determined using the eqn. 28

$$\Delta X_{t+1} = (sS_i + aA_i + cC_i + fF_i + eE_i) + w\Delta X_i \text{... (28)}$$

Where: $s$ shows the separation weight, $S_i$ indicates the separation of the *i*th individual, $a$ is the alignment weight, $A_i$ is the alignment of the *i*th individual, $c$ as the cohesion weight, $C_i$ is the cohesion of the *i*th individual, $f$ as the food factor, $F_i$ is the food source of the *i*th individual, $e$ is the enemy factor, $E_i$ indicates the position of enemy for the *i*th individual, $w$ is the inertia weight, and $t$ as the iteration counter (Darwish, 2018).

The position vectors were calculated as eqn. 29

$$\Delta X_{t+1} = X_t + \Delta X_{t+1} \text{..... (29)}$$

During optimization phase, various exploitative and explorative behaviors could be gained through separation, alignment, cohesion, food, and enemy factors. Neighboring of dragonflies were important, thus neighborhood of artificial dragonflies within a specific radius was assumed. When there were no neighboring solutions, artificial dragonflies used Lévy flight to improve the randomness, exploration, and stochastic behavior (Darwish, 2018).

The process of optimization was started by establishing a set of random solutions. The identified random values in the upper and lower bounds of the variables were initialized by the step and position vectors. The step and position of each dragonfly were updated. The Euclidean distance of the neighboring dragonfly and their N will be calculated to update the $X$ and $\Delta X$ vectors. The process of updating the position is continued repetitively until it reaches the satisfaction of the end criterion (Darwish, 2018).

**Moth Flame Optimization (MFO)**

In the mathematical model of MFO algorithm, the candidate solutions were typified by the moths and their position in the search space which represented the variables (Mirjalili, 2015). Thereafter, moths would be able to fly on hyperdimensional space which was described by the matrix form:

$$M = \begin{bmatrix} m_{1,1} & m_{1,2} & \cdots & \cdots & m_{1,d} \\ m_{2,1} & m_{2,2} & \cdots & \cdots & m_{2,d} \\ \vdots & \vdots & \vdots & \vdots & \vdots \\ m_{n,1} & m_{n,2} & \cdots & \cdots & m_{n,d} \end{bmatrix} \quad \text{..... (30)}$$

Where: *n* represents the number of moths and *d* represents the number of variables.

To store the values of the corresponding fitness, there is an array that can be used and considered for every moth:

$$OM = \begin{bmatrix} OM_1 \\ OM_2 \\ \vdots \\ OM_n \end{bmatrix} \quad \text{..... (31)}$$

Each moth's position vector was passed to the objective function and its output was assigned as the fitness values of the corresponding moth (Darwish, 2018). Meanwhile, flame (F) was similar to matrix M, which was an important element in the algorithm, represented by:

$$F = \begin{bmatrix} F_{1,1} & F_{1,2} & \cdots & \cdots & F_{1,d} \\ F_{2,1} & F_{2,2} & \cdots & \cdots & F_{2,d} \\ \vdots & \vdots & \vdots & \vdots & \vdots \\ F_{n,1} & F_{n,2} & \cdots & \cdots & F_{n,d} \end{bmatrix} \quad \text{..... (32)}$$

To store the corresponding values of fitness function for Flames, the following array was considered:

$$OF = \begin{bmatrix} OF_1 \\ OF_2 \\ \vdots \\ OF_n \end{bmatrix} \quad \text{..... (33)}$$

As identified, moths and flames were both considered solutions but varied on the process they were being treated and updated in every iteration. As actual search agents, moths moved around the search space, while flames were their best positions obtained during the activity (Darwish, 2018; Mirjalili, 2015).

For this algorithm, the optimal value was described using the mathematical form (eqn. 34-37)

$$MFO=(I,P,T) \quad \text{..... (34)}$$

Where $I$ represent moth population generated randomly and the fitness values given by:

$$I : \theta \rightarrow \{M,OM\} \quad \text{..... (35)}$$

*P* represents activity of the moths around the search space and represented by:

$$\mathrm{P} : \mathrm{M} \rightarrow \mathrm{M} \quad \text{..... (36)}$$

and finally, *T* as the termination criterion functions of either true or false, and was defined by:

$$\mathrm{T} : \mathrm{M} \rightarrow \{\mathrm{true},\mathrm{false}\} \quad \text{..... (37)}$$

The MFO algorithm's general scheme was represented by the functions $I$, $P$, and $T$ (Darwish, 2018; Mirjalili, 2015).

The configured system parameters for GWO, WOA, DA, and MFO were the following: $10\ cm \leq x_1 \leq 30$ cm , $222\ \mu mol/m^2/s \leq x_2 \leq 3112\ \mu mol/m^2/s$ , $1097\ \mu mol/m^2/s \leq x_3 \leq 26660\ \mu mol/m^2/s$ and $875\ \mu mol/m^2 s \leq x_4 \leq 23548\ \mu mol/m^2/s$ Fifty (50) repeating simulations were done for each algorithm.

## RESULTS AND DISCUSSION

### Artificial Light Properties and Light Spectrum

Light intensity and proximity were the basis of each monochromatic light spectrum photosynthetic capacity. The highest intensity was produced by the white light for 30, 20, and 10 cm proxinities with 380.956, 544.663, and 1131.480 µmol/m$^2$/s, respectively. The violet spectrum produced the lowest light intensity of only 37.967, 63.143, and 116.264 µmol/m$^2$/s for 30, 20, and 10 cm proximities, respectively (Fig. 3) (Concepcion et al., 2021; Bautista, et al., 2022).

The lowest visible to infrared radiation ratio (Vis/IR) was from violet light with 3.941, 3.840, and 3.797 for 30, 20, and 10 cm distances, respectively. Blue light gave the highest Vis/IR with 8.751, 8.531, and 8.254 for 30, 20, and 10 cm proximities, respectively. These results also showed that farther proximity gave a higher value of Vis/IR (Fig. 4) (Concepcion et al., 2021; Bautista, et al., 2022).

### Photosynthetic and Respiration Rates

Results showed that the highest photosynthetic rate for both stage of aquaponic lettuce was induced by the white light in the 30, 20, and 10 cm distances with the average of 0.162, 0.162, and 0.111 disks/min, respectively. Green light gave the lowest photosynthetic rate of 0.083 disks/min for 30 cm, and 0.075 disks/min for 20 cm, while orange light with 0.076 disks/min for the 10 cm proximity. Closer distance exhibited lower photosynthetic rate due to a low Vis/IR (Fig. 5) (Concepcion et al., 2021; Bautista, et al., 2022).

In addition, artificial white light also gave the highest respiration rate for 30, 20, and 10 cm light proximities with an average of 0.030, 0.027, and 0.029 disks/min, respectively. On the other hands, green light also produced the lowest respiration rate

of 0.026, 0.024, and 0.025 disks/min for 30, 20, and 10cm proximities, respectively (Fig. 6) (Concepcion et al., 2021; Bautista, et al., 2022).

**Optimized Artificial Light Properties**

Bioinspired optimization algorithms, namely grey wolf optimization (GWO), whale optimization algorithm (WOA), dragonfly algorithm (DA), and moth flame optimization (MFO) were used for evapotranspiration rate optimization of both head development-stage and harvest-stage aquaponic lettuce after successfully converging using 1000 iterations.

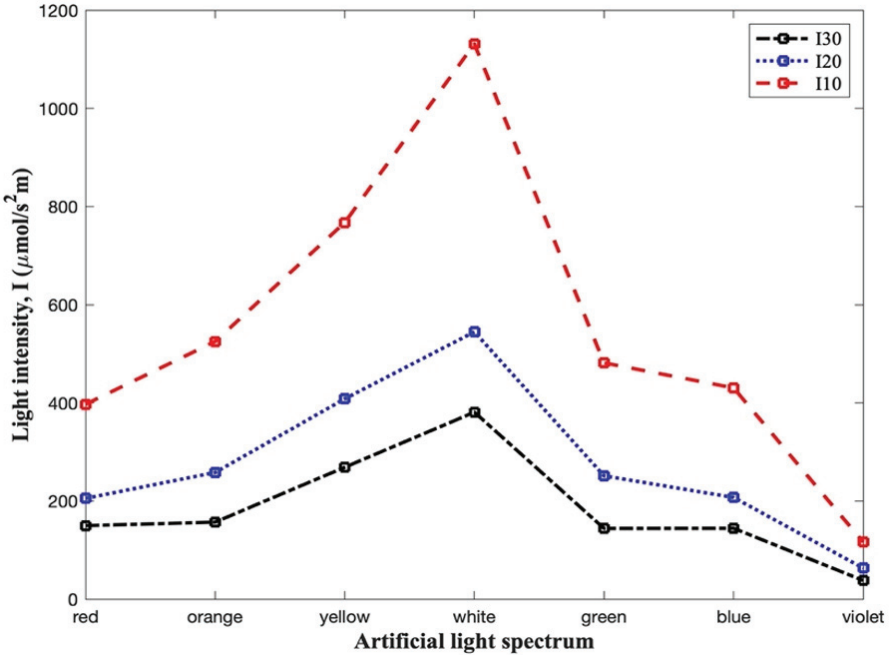


**Fig. 3.** Light intensity (I) based on the spectrum and distance from the light source: 30, 20, and 10 cm

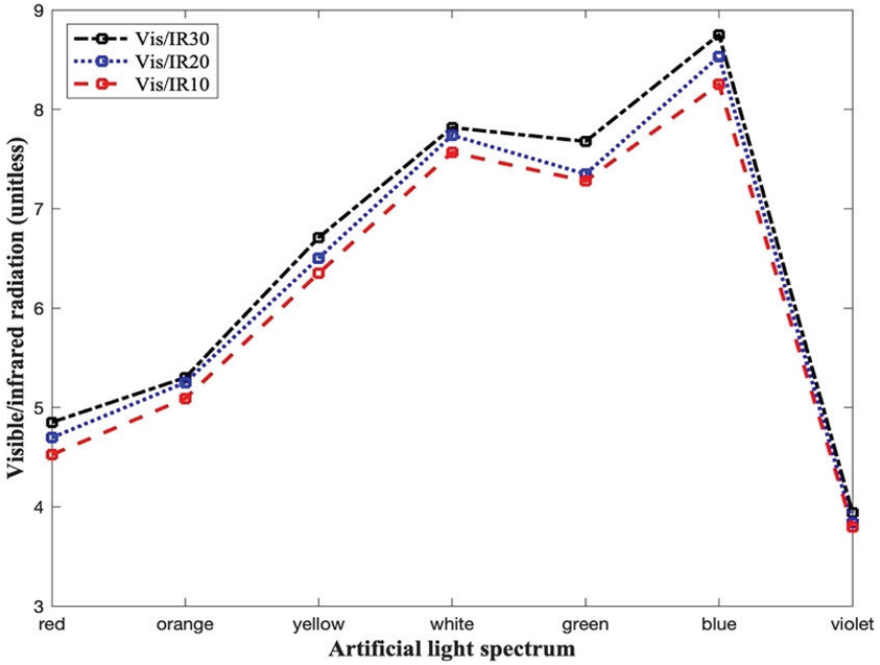


**Fig. 4.** Visible and infrared radiation ratio (Vis/IR) based on spectrum and distance from the light source: 30, 20, and 10 cm

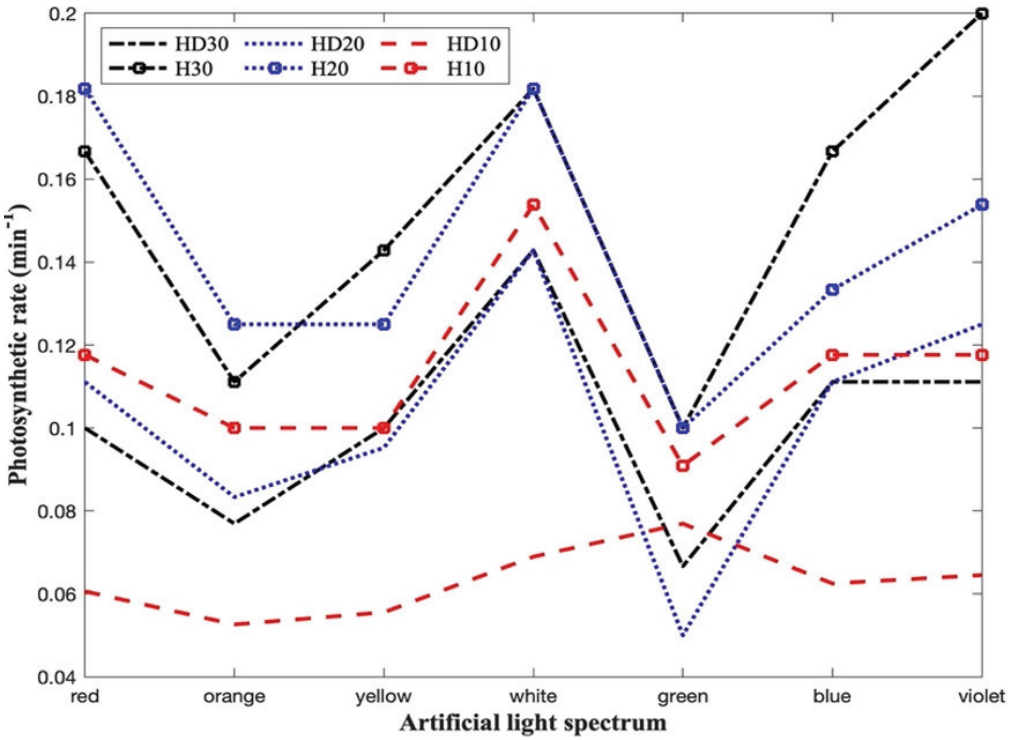


**Fig. 5.** Photosynthetic rate based on spectrum and distance from the light source: 30, 20, and 10 cm

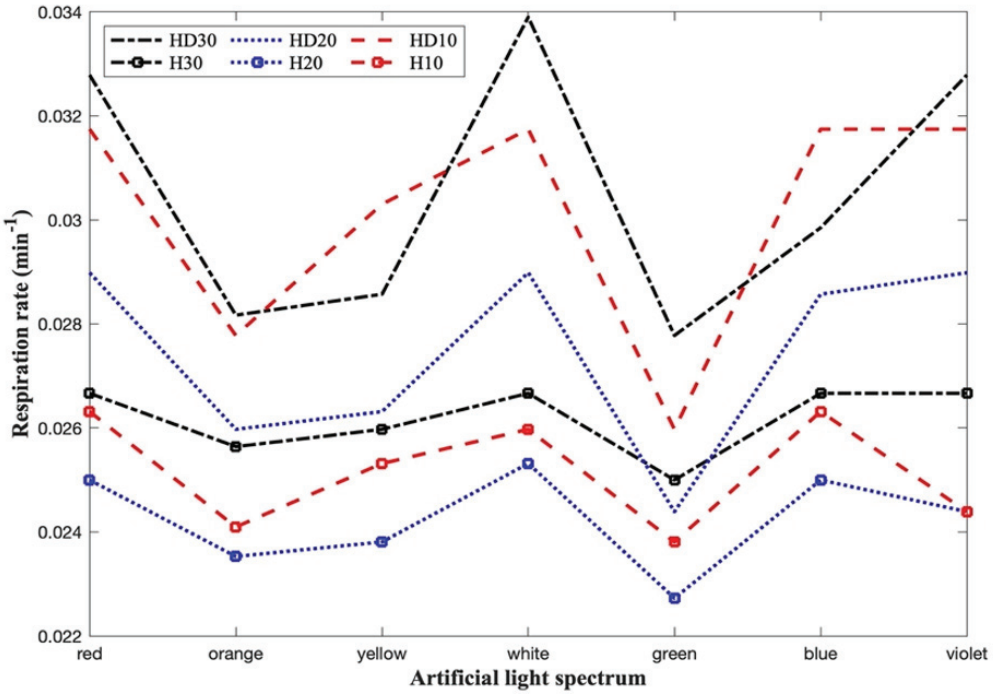


**Fig. 6.** Respiration rate based on spectrum and distance from the light source: 30, 20, and 10 cm

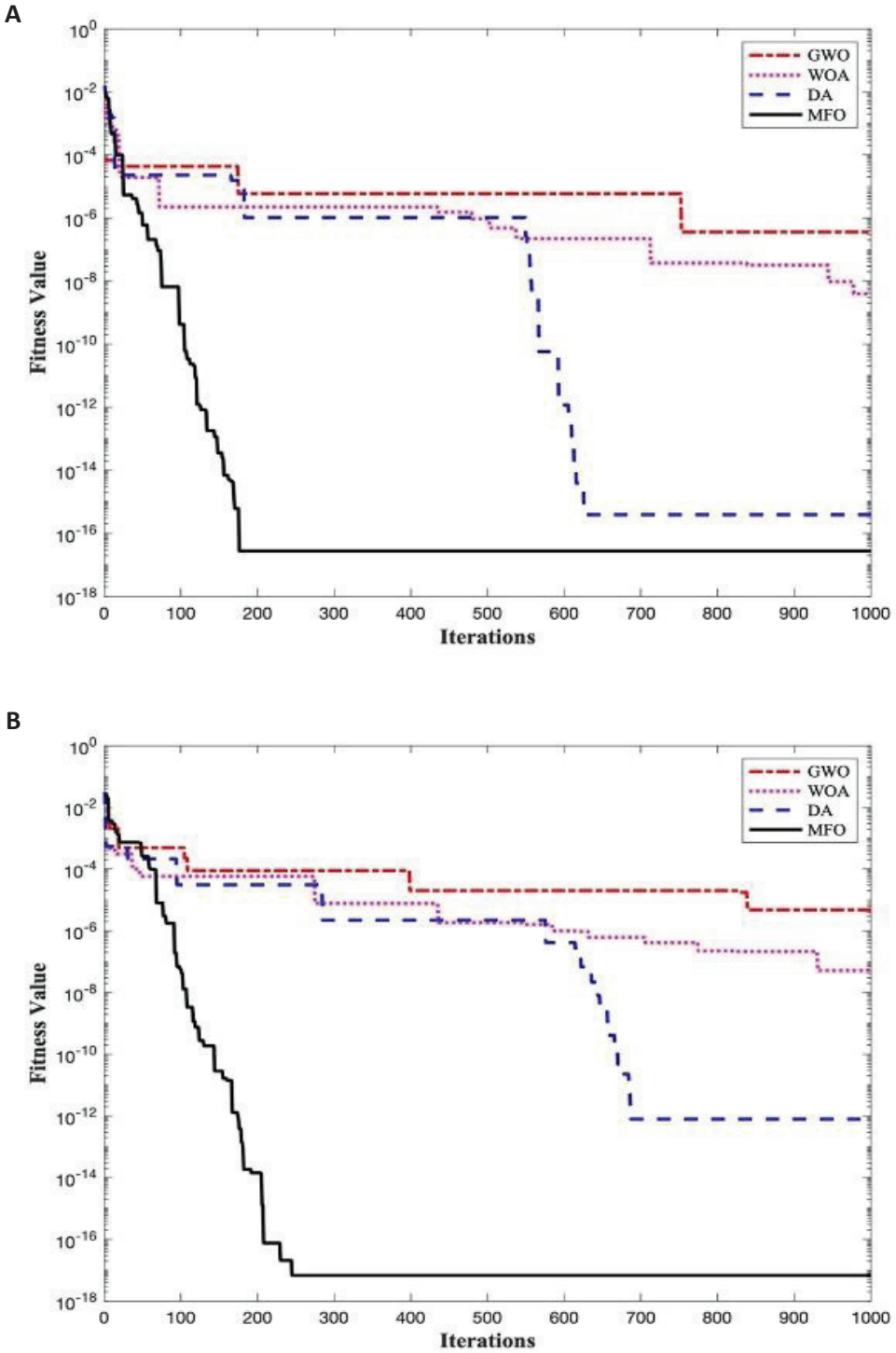


**Fig. 7.** Convergence curve of GWO, WOA, DA, and MFO for 1000 iterations in determining the optimum combined light properties for minimum evapotranspiration rate of (a) head development-stage lettuce and (b) harvest-stage lettuce during light period

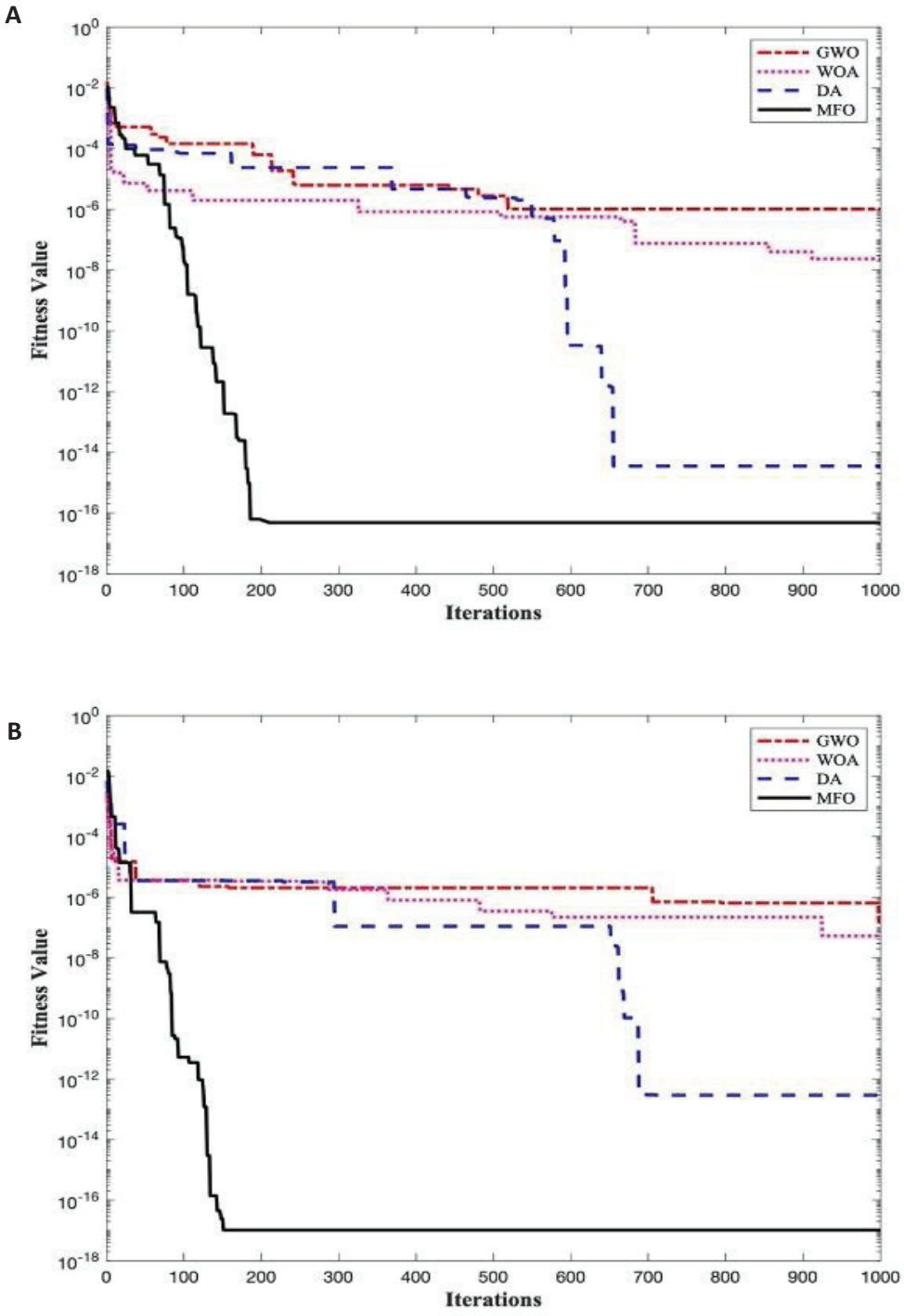


**Fig. 8.** Convergence curve of GWO, WOA, DA, and MFO for 1000 iterations in determining the optimum combined light properties for minimum evapotranspiration rate of (a) head development-stage lettuce and (b) harvest-stage lettuce during dark period

Fig. 7a showed the determined optimum combined light properties for minimum evapotranspiration rate of head development-stage lettuce during light period. MFO gave the optimum values of 16.030 cm distance from the light source, with a light intensity of 13544.84 μmol/m$^2$/s, and visible and infrared radiations of 3647.538 μmol/m$^2$/s and 1084.541 μmol/m$^2$/s, respectively (Table 1).

MFO also gave the optimized light properties for minimizing the evapotranspiration rate of harvest-stage lettuce during light period (Fig. 7b) with 18.572 cm, a light intensity of 6137.475 μmol/m$^2$/s, visible radiation of 8861.246 μmol/m$^2$/s, and infrared radiation of 1166.030 μmol/m$^2$/s (Table 2).

Moth Flame Optimization algorithm also exhibited the optimized artificial light properties for both aquaponic lettuce stages during dark-period respiration reaction (Fig. 8a and Fig. 8b).

Table 3 showed the optimum values with 17.904 cm distance, 14444.156 μmol/m$^2$/s light intensity, 1035.466 μmol/m$^2$/s infrared radiation, and 9014.807 μmol/m$^2$/s visible radiation for the head development-stage lettuce.

Finally, determined best global solution for harvest-stage lettuce were 18.710 cm proximity from the light source, and light intensity, visible radiation, and infrared radiation of 20363.843 μmol/m$^2$/s, 2117.213 μmol/m$^2$/s, and 2886.614 μmol/m$^2$/s, respectively (Table 4).

Results of the study indicated that head development-stage lettuce required higher light intensity and lower Vis/IR than harvest-stage lettuce during light period. On the other hand, harvest-stage lettuce needed higher light intensity and lower Vis/IR than head development stage-lettuce during dark period.

Based on the generated optimal artificial light properties using bio-inspired algorithms when under dark-period respiration reaction, head development-stage lettuce required highest Vis/IR while harvest-stage lettuce required the lowest.

Prior study noted the importance of optimizing light intensity for accurate estimation of water productivity that would become imperative in planning ang managing irrigation practice. Results of this study showed that growth parameters such as fresh weigh, dry weight, and leaf area were improved by increasing light intensity together with carbon dioxide concentration (Esmaili et al., 2021). Another study about dependency of growth of lettuce plants to light intensity emphasized that exposure to higher light intensities causing faster development of photosynthesis system was dependent on the leaf developmental stages (Ghorbanzadeh et al., 2020). A recent study conducted experiments of exposing lettuce crops to different artificial light cycles to establish an effective leaf area model using thermal effectiveness and photosynthetically active radiation (TEP) method. Result showed that light cycle influenced lettuce leaf area significantly, where 12-h/12-h (light/dark) treatment resulted to better lettuce growth (Hang et al., 2019).

Effects of evapotranspiration in the circulation of atmosphere had a great impact on plant growth and yield and was proven as an effective basis for efficient irrigation management (Zhangzhong et al., 2023). Using LEDs as source of artificial light was more energy efficient than other light sources and could be controlled easily for optimum light intensity to improve plant growth. A recent study also used LED as artificial light source and proved the positive effects of optimizing light intensity for red lettuce (Modarelli et al., 2022).

**Table 1.** Optimal artificial light properties generate using bio-inspired algorithms for head development-stage lettuce during light period

| Model | Distance (cm) | Infrared radiation (μmol/m$^2$/s) | Light intensity (μmol/m$^2$/s) | Visible radiation (μmol/m$^2$/s) |
|---|---|---|---|---|
| GWO | 15.011 | 985.991 | 11952.286 | 3704.909 |
| WOA | 16.152 | 1055.041 | 12687.129 | 3233.738 |
| DA | 19.152 | 1285.500 | 10648.768 | 3226.788 |
| **MFO** | **16.030** | **1084.541** | **13544.84** | **3647.538** |

Remarks: GWO = grey wolf optimization, WOA = whale optimization algorithm, DA = dragonfly algorithm, MFO = moth flame optimization

**Table 2.** Optimal artificial light properties generate using bio-inspired algorithms for harvest-stage lettuce during light period

| Model | Distance (cm) | Infrared radiation (μmol/m²/s) | Light intensity (μmol/m²/s) | Visible radiation (μmol/m²/s) |
|---|---|---|---|---|
| GWO | 17.816 | 881.710 | 5165.641 | 6957.088 |
| WOA | 15.758 | 875.290 | 4263.256 | 5354.158 |
| DA | 18.209 | 1411.283 | 7139.383 | 9103.532 |
| **MFO** | **18.572** | **1166.030** | **6137.475** | **8861.246** |

Remarks: GWO = grey wolf optimization, WOA = whale optimization algorithm, DA = dragonfly algorithm, MFO = moth flame optimization

**Table 3.** Optimal artificial light properties generate using bio-inspired algorithms for head development-stage lettuce during dark period

| Model | Distance (cm) | Infrared radiation (μmol/m²/s) | Light intensity (μmol/m²/s) | Visible radiation (μmol/m²/s) |
|---|---|---|---|---|
| GWO | 16.599 | 832.707 | 12609.167 | 8154.135 |
| WOA | 16.749 | 1003.055 | 10511.929 | 7283.245 |
| DA | 21.562 | 1399.441 | 13733.691 | 8153.700 |
| **MFO** | **17.904** | **1035.466** | **14444.156** | **9014.807** |

Remarks: GWO = grey wolf optimization, WOA = whale optimization algorithm, DA = dragonfly algorithm, MFO = moth flame optimization

**Table 4.** Optimal artificial light properties generate using bio-inspired algorithms for harvest-stage lettuce during dark period

| Model | Distance (cm) | Infrared radiation (μmol/m²/s) | Light intensity (μmol/m²/s) | Visible radiation (μmol/m²/s) |
|---|---|---|---|---|
| GWO | 18.161 | 2919.300 | 19642.162 | 1979.148 |
| WOA | 25.476 | 2895.791 | 23130.000 | 4598.733 |
| DA | 23.274 | 2893.193 | 21906.675 | 3857.867 |
| **MFO** | **18.710** | **2886.614** | **20363.843** | **2117.213** |

Remarks: GWO = grey wolf optimization, WOA = whale optimization algorithm, DA = dragonfly algorithm, MFO = moth flame optimization

Findings of this research provided valuable insights into the combinational regulation of artificial light properties for head development-stage and harvest-stage lettuce under light-dependent photosynthetic reaction and dark-period respiration reaction for improving growth of lettuce crop in greenhouse and plant factory.

## CONCLUSION

This study showed that hybrid multigene symbolic regression genetic programming and moth flame optimization algorithm (MSRGP-MFO) could establish the ideal values of artificial light properties to minimize evapotranspiration rate of both the head development and harvest-stage lettuce under light-dependent photosynthetic reaction and dark-period respiration reaction. Head development-stage lettuce under light period needed the minimum obtained optimal distance of 16.030 cm from the light source. On the other hands, harvest-stage lettuce needed lowest artificial light intensity of 6137.475 μmol/m²/s when exposed to light. In terms of the visible to infrared radiation ratio, head development-stage lettuce under dark period needed the maximum 8.706 while harvest-stage lettuce needed only a Vis/IR ratio of 0.733. Grey wolf algorithm, whale optimization algorithm and dragonfly algorithm also gave best solutions for low values of evapotranspiration rate. For future studies, it is recommended to consider the color of the artificial

light together with other properties in determining the minimum evapotranspiration for improving growth of lettuce in controlled environment. Based on this optimized environment, quantification of nutrient use can be explored in identifying impact to lettuce growth.

## ACKNOWLEDGEMENTS

The authors highly recognize the support of the Department of Science and Technology's (DOST) Engineering Research and Development for Technology (ERDT) and the Intelligent Systems Laboratory of the De La Salle University, Philippines.

## REFERENCES

Bautista, M., Alejandrino, J., Alajas, O., Mendigoria, C., Concepcion R., Dadios, E., Bandala, A., & Vicerra, R. (2022). 8-10-Gene Expression-Based aquaponic lettuce evapotranspiration optimization based on photosynthetic light properties. *Proceedings of the International Conference on Intelligent Computing & Optimization (ICO2022),* 674 – 685. https://doi.org/10.1007/978-3-031-19958-5_64

Benke, K., & Tomkins, B. (2017). Future food-production systems: Vertical farming and controlled-environment agriculture. *Sustainability: Science, Practice and Policy*, *13*(1), 13–26. https://doi.org/10.1080/15487733.2017.1394054

Cammarisano, L., Donnison, I. S., & Robson, P. R. H. (2019). Producing enhanced yield and nutritional pigmentation in Lollo Rosso through manipulating the irradiance, duration, and periodicity of LEDs in the visible region of light. *Frontiers in Plant Science*, *11*, 2019. https://doi.org/10.3389/FPLS.2020.598082/BIBTEX

Camejo, D., Frutos, A., Mestre, T. C., del Carmen Piñero, M., Rivero, R. M., & Martínez, V. (2020). Artificial light impacts the physical and nutritional quality of lettuce plants. *Horticulture Environment and Biotechnology, 61*(1), 69–82. https://doi.org/10.1007/S13580-019-00191-Z

Chen, X. li, Wang, L. chun, Li, T., Yang, Q. chang, & Guo, W. zhong. (2019). Sugar accumulation and growth of lettuce exposed to different lighting modes of red and blue LED light. *Scientific Reports, 9*(1). https://doi.org/10.1038/S41598-019-43498-8

Chen, X. li, Yang, Q. chang, Song, W. pin, Wang, L. chun, Guo, W. zhong, & Xue, X. zhang. (2017). Growth and nutritional properties of lettuce affected by different alternating intervals of red and blue LED irradiation. *Scientia Horticulturae*, *223*, 44–52. https://doi.org/10.1016/J.SCIENTA.2017.04.037

Concepcion, R., Dadios, E., Bandala, A., Cuello, J., & Kodama, Y. (2021). Hybrid genetic programming and multiverse-based optimization of pre-harvest growth factors of aquaponic lettuce based on chlorophyll concentration. *International Journal on Advanced Science, Engineering and Information Technology*, *11*(6), 2128–2138. https://doi.org/10.18517/IJASEIT.11.6.14991

Darwish, A. (2018). Bio-inspired computing: Algorithms review, deep analysis, and the scope of applications. *Future Computing and Informatics Journal*, *3*(2), 231–246. https://doi.org/10.1016/J.FCIJ.2018.06.001

Esmaili, M., Aliniaeifard, S., Mashal, M., Vakilian, K. A., Ghorbanzadeh, P., Azadegan, B., Seif, M., & Didaran, F. (2021). Assessment of adaptive neuro-fuzzy inference system (ANFIS) to predict production and water productivity of lettuce in response to different light intensities and CO2 concentrations. *Agricultural Water Management*, *258*, 107201. https://doi.org/10.1016/J.AGWAT.2021.107201

Ghorbanzadeh, P., Aliniaeifard, S., Esmaeili, M., Mashal, M., Azadegan, B., & Seif, M. (2020). Dependency of Growth, water use efficiency, chlorophyll fluorescence, and stomatal characteristics of lettuce plants to light intensity. *Journal of Plant Growth Regulation*, *40*(5), 2191–2207. https://doi.org/10.1007/S00344-020-10269-Z

Hang, T., Lu, N., Takagaki, M., & Mao, H. (2019). Leaf area model based on thermal effectiveness and photosynthetically active radiation in lettuce grown in mini-plant factories under different light cycles. *Scientia Horticulturae*, *252*, 113–120. https://doi.org/10.1016/J.SCIENTA.2019.03.057

Izzo, L. G., Mickens, M. A., Aronne, G., & Gómez, C. (2021). Spectral effects of blue and red light on growth, anatomy, and physiology of lettuce. *Physiologia Plantarum*, *172*(4), 2191–2202. https://doi.org/10.1111/PPL.13395

Ke, X., Yoshida, H., Hikosaka, S., & Goto, E. (2021). Optimization of photosynthetic photon flux density and light quality for increasing radiation-use efficiency in dwarf tomato under LED light at the vegetative growth stage. *Plants*, *11*(1), 121. https://doi.org/10.3390/PLANTS11010121

Kump, B. (2020). The role of far-red light (FR) in photomorphogenesis and its use in greenhouse plant production. *Acta Agriculturae Slovenica*, *116*(1), 93–105. https://doi.org/10.14720/AAS.2020.116.1.1652

Kwack, Y., An, S., & Kim, S. K. (2021). Development of growth model for grafted hot pepper seedlings as affected by air temperature and light intensity. *Sustainability*, *13*(11), 5895. https://doi.org/10.3390/SU13115895

Lee, M. J., Son, K. H., & Oh, M. M. (2016). Increase in biomass and bioactive compounds in lettuce under various ratios of red to far-red LED light supplemented with blue LED light. *Horticulture, Environment, and Biotechnology*, *57*(2), 139–147. https://doi.org/10.1007/S13580-016-0133-6

Loconsole, D., Cocetta, G., Santoro, P., & Ferrante, A. (2019). Optimization of LED lighting and quality evaluation of Romaine lettuce grown in an innovative indoor cultivation system. *Sustainability*, *11*(3), 841. https://doi.org/10.3390/SU11030841

Marcos, L., & Mai, K. V. (2020). Light spectra optimization in indoor plant growth for internet of things. *Proceedings of the International IOT, Electronics and Mechatronics Conference*. https://doi.org/10.1109/IEMTRONICS51293.2020.9216421

Mirjalili, S. (2015). Moth-flame optimization algorithm: A novel nature-inspired heuristic paradigm. *Knowledge-Based Systems*, *89*, 228–249. https://doi.org/10.1016/J.KNOSYS.2015.07.006

Mirjalili, S., & Lewis, A. (2016). The Whale Optimization Algorithm. *Advances in Engineering Software*, *95*, 51–67. https://doi.org/10.1016/J.ADVENGSOFT.2016.01.008

Modarelli, G.C., Paradiso, R., Arena, C., De Pascale, S., & Van Labeke, M.-C. (2022). High light intensity from blue-red LEDs enhance photosynthetic performance, plant growth, and optical properties of red lettuce in controlled environment. *Horticulturae*, *8*(2), 114. https://doi.org/10.3390/horticulturae8020114

Mohamed, S. J., Rihan, H. Z., Aljafer, N., & Fuller, M. P. (2021). The impact of light spectrum and intensity on the growth, physiology, and antioxidant activity of lettuce (*Lactuca sativa* L.). *Plants* , *10*(10). https://doi.org/10.3390/PLANTS10102162

Monga, P., Sharma, M., & Sharma, S. K. (2021). A comprehensive meta-analysis of emerging swarm intelligent computing techniques and their research trend. In *Journal of King Saud University - Computer and Information Sciences*. King Saud bin Abdulaziz University. https://doi.org/10.1016/j.jksuci.2021.11.016

National Economic Development Authority. (2017). *Updated Philippine Development Plan 2017-2022*. Retrieved from https://pdp.neda.gov.ph/updated-pdp-2017-2022/

Périard, Y., Caron, J., Lafond, J. A., & Jutras, S. (2015). Root water uptake by Romaine lettuce in a muck soil: Linking tip burn to hydric deficit. *Vadose Zone Journal, 14*(6), vzj2014.10.0139. https://doi.org/10.2136/VZJ2014.10.0139

Tarakanov, I. G., Tovstyko, D. A., Lomakin, M. P., Shmakov, A. S., Sleptsov, N. N., Shmarev, A. N., Litvinskiy, V. A., & Ivlev, A. A. (2022). Effects of light spectral quality on photosynthetic activity, biomass production, and carbon isotope fractionation in lettuce, *Lactuca sativa* L., Plants. *Plants (Basel, Switzerland), 11*(3). https://doi.org/10.3390/PLANTS11030441

Urairi, C., Shimizu, H., Nakashima, H., Miyasaka, J., & Ohdoi, K. (2017). Optimization of light-dark cycles of *Lactuca sativa* L. in plant factory. *Environmental Control in Biology*, *55*(2), 85–91. https://doi.org/10.2525/ECB.55.85

Valenzuela, I., Baldovino, R., Bandala, A., & Dadios, E. (2018). Pre-harvest factors optimization using genetic algorithm for lettuce. *Journal of Telecommunication, Electronic and Computer Engineering (JTEC)*, *10*(1–4), 159–163. https://jtec.utem.edu.my/jtec/article/view/3610

Valenzuela, I. C., Baldovino, R. G., Bandala, A. A., & Dadios, E. P. (2017). Optimization of photosynthetic rate parameters using Adaptive Neuro-Fuzzy Inference System (ANFIS). *2017 International Conference on Computer and Applications*, 129–134. https://doi.org/10.1109/COMAPP.2017.8079734

Zhangzhong, L., Gao, H., Zheng, W., Wu, J., Li, J., & Wang, D. (2023). Development of an evapotranspiration estimation method for lettuce via mobile phones using machine vision: Proof of concept. *Agricultural Water Management*, *275,* 108003. https://doi.org/10.1016/j.agwat.2022.108003

Zou, J., Zhou, C. bo, Xu, H., Cheng, R. feng, Yang, Q. chang, & Li, T. (2020). The effect of artificial solar spectrum on growth of cucumber and lettuce under controlled environment. *Journal of Integrative Agriculture*, *19*(8), 2027–2034. https://doi.org/10.1016/S2095-3119(20)63209-9

Zou, T., Huang, C., Wu, P., Ge, L., & Xu, Y. (2020). Optimization of artificial light for spinach growth in plant factory based on orthogonal test. *Plants*, *9*(4), 490. https://doi.org/10.3390/PLANTS9040490